MNE 19 (2023) 100199

Contents lists available at ScienceDirect

Micro and Nano Engineering

journal homepage: www.sciencedirect.com/journal/micro-and-nano-engineering

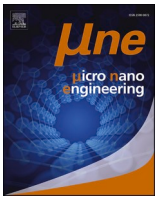

Novel design for a microfluidic-based platform for yeast replicative lifespan (RLS) analysis

Georgia D. Kaprou [a,**], Abhay Andar [b,c], Pranjul Shah [a], Carole L. Linster [a], Nicole Paczia [a,d,*]

[a] Luxembourg Centre for Systems Biomedicine, University of Luxembourg, Belvaux 4367, Luxembourg
[b] Center for Advanced Sensor Technology, University of Maryland Baltimore County, Baltimore, MD 21250, United States
[c] Potomac Photonics Inc., BWTech Parkway South Campus, 1450 South Rolling Road, Baltimore, MD 20008, United States of America
[d] Core Facility for Metabolomics and Small Molecule Mass Spectrometry, Max Planck Institute for Terrestrial Microbiology, Marburg, Germany

ARTICLE INFO

Keywords:
Microfluidics
Yeast
Photolithography
Single cell trapping
Replicative lifespan

ABSTRACT

Microfluidic devices hold enormous potential for the development of cost-effective and faster alternatives to existing traditional methods across life science applications. Here we demonstrate the feasibility of fabricating a microfluidic device by means of photolithography comprising a single cell trap, a delay structure and a chamber defined by micropillars. This device is aimed to be used for biological applications such as replicative lifespan determination (RLS) of yeast cells, where single cell trapping, and cell counting are essential. The novelty of the present work lies on the integration of the above-mentioned microfluidic structures in a single device by means of the established method of photolithography by fine-tuning critical parameters needed to achieve the desired high aspect ratio (1:5) employing commercially available resins. The fine-tuning of the fabrication parameters in combination with appropriately selected resins allows for patterning reproducibly micron-sized features. The design of the proposed device ultimately aims at replacing the very cumbersome assays still commonly used today for RLS determination in budding yeast by a methodology that is drastically simpler and more time efficient.

1. Introduction

Microfluidic technology, emerged 40 years ago [1], has by now become a mature and well-established technology, providing an attractive toolbox for the manipulation and handling of fluid samples, particles and cells [2]. It has evolved through the interplay between technology and biomedical sciences to progressively enable miniaturization of routine analyses and conventional diagnostics in microfluidic devices. Developments in microfluidics require multidisciplinary efforts from fields including physics, biology, chemistry, and engineering and provide benefits to various areas in engineering and science, ranging from aerospace engineering [3] to biomedical applications [4]. Microfluidics enables the miniaturization, integration, automation, and portability of biochemical analysis as well as the fabrication of microdevices with precisely controlled features and functions [5]. Thus, microfluidic devices constitute new platforms occasionally enabling high-throughput processing and offering enhanced potential for automation [3].

Microfluidics allows the manipulation and controlling of fluids and particles at micron and submicron scale using microchannels and/or microchambers with dimensions of tens to hundreds of micrometers and are thus well-suited for the manipulation of cells and biomolecules [4]. In the early 1990s, microelectronic technology began to gain popularity as a means of fabrication for miniaturized devices for analytical chemistry systems such as chromatography and capillary electrophoresis. Since then, microfluidics has advanced tremendously and has revolutionized conventional laboratory processes and analytical techniques due to its potential to substantially lessen the sample volumes, the duration, and the cost while increasing the sensitivity of the carried-out processes and offering excellent control over reaction conditions [5]. Microfluidic tools coupled with advanced molecular, bioinformatics, and imaging techniques compose a versatile and adjustable toolbox that

* Corresponding author at: Luxembourg Centre for Systems Biomedicine, University of Luxembourg, Belvaux 4367, Luxembourg, Core Facility for Metabolomics and Small Molecule Mass Spectrometry, Max Planck Institute for Terrestrial Microbiology, Marburg, Germany.
** Corresponding author.
E-mail addresses: georgia.kaprou@uni.lu (G.D. Kaprou), aandar@potomac-laser.com (A. Andar), pranjul.shah@uni.lu (P. Shah), carole.linster@uni.lu (C.L. Linster), nicole.paczia@mpi-marburg.mpg.de (N. Paczia).

https://doi.org/10.1016/j.mne.2023.100199
Received 14 December 2022; Received in revised form 17 April 2023; Accepted 5 May 2023
Available online 6 May 2023

life science researchers enthusiastically adapt and adopt to address challenges and long-standing questions in their fields. In more detail, microfluidics allows scientists to deconstruct perplexing biological relationships through the representation of the biological microenvironment in a tailored and customized fashion, which can be precisely controlled and closely monitored by employing, for instance, real-time high-resolution imaging. The ample range of possible biological applications for microfluidics, encompassing high-throughput drug screening [6], drug delivery [7], nucleic acid amplification [8,9], cell sorting [10], single cell or biomolecule analysis and manipulation [11], sequencing [12,13], as well as biosensing [14] and diagnostics [15,16], is the main driving force behind the swift development of this technology.

A wide and diverse repertoire of fabrication methods can be chosen in order to manufacture microfluidic devices bearing the desired features in terms of geometry, shape, and size [17]. The microfabrication technology methods include reactive ion etching [18], plasma etching [19], wet etching [20], conventional machining [21], photolithography [22], soft lithography [23], injection molding [24], hot embossing [25], laser ablation [26], 3D printing [27], nanoimprint lithography [28], electron beam lithography [29], and extreme ultraviolet lithography [30,31]. The choice of fabrication method depends on various factors such as the availability of equipment and technologies, speed, cost, patterning capabilities (i.e. feature size, resolution) as well as the substrate material [32]. The selection of the optimal material is considered an essential step for device fabrication in microfluidic applications, since the properties of the selected materials (e.g. transparency, durability, biocompatibility, ease of fabrication, chemical compatibility with reagents, and temperature tolerance) can critically affect the outcomes of the fabrication processes [17].

The most used substrates for microfluidic device manufacturing include glass, silicon, polymers, and metals. Silicon is one of the dominant materials used due to its thermostability, chemical compatibility, ready availability, design flexibility, ease of fabrication, semiconducting properties as well as the possibility of applying surface modifications [33]. Nevertheless, silicon possesses several disadvantages such as the opacity, which interferes with optical detection, the fragility, which hampers the integration with other active components (e.g. pumps and valves), and the relatively high cost [34]. As for the properties of glass, it is chemically inert, biocompatible, thermostable, rigid, electrically insulating and allows facile surface functionalization. Thus, glass is suitable for fabricating microreactors for chemical reactions requiring extreme conditions (e.g., aggressive solvents, high temperatures). Unlike silicon, glass possesses the advantages of excellent optical transparency (suitable for optical detection) and the possibility of incorporating active components. However, glass microfabrication is time-consuming and usually demands cleanroom facilities [35]. The concept of employing polymers in microfluidics was introduced in the 1990s [36]. Polymers enable inexpensive and rapid prototyping and allow high-density integration of components (e.g., valves) on chips, thus enabling complex and parallel fluid manipulation. Polymers offer a wide range of physical and chemical properties. In terms of manufacturing, polymer-based microfluidic devices are, in general, amenable to mass production processes (i.e., injection-molding, hot-embossing, and roll-to-roll). Moreover, polymers can be transparent or semitransparent, thus offering good optical properties and allowing for an optical detection [37]. Finally, metals are widely accessible, cheap, easy to machine and can endure high pressures, high heat loads, and toxic chemicals. The most commonly used metals for microfluidics are copper, aluminum, and iron, usually found in alloys [17].

Aging is a major risk factor for a wide range of diseases including diabetes, neurodegenerative disorders, cardiovascular diseases, and cancer. The increasing aging population causes a huge socioeconomic burden which is mainly attributed to age-associated diseases [38].

The single cell organism *Saccharomyces cerevisiae* is an important model for studying the molecular mechanisms of aging in eukaryotic cells. It has played a pivotal role in the understanding of basic cellular processes such as cell cycle regulation [39,40], intracellular trafficking [41,42], protein folding regulation [40,43], and many others. Most benefits of using yeast are based on its short generation time, convenient and cheap experimental setups, straightforward genetic approaches, and, more recently, high-throughput methodologies. Additionally, yeast presents relatively high genetic conservation with mammals including humans, which makes it effective to model human diseases [44].

As yeast is proliferating in an unsymmetrical way, there are two different approaches to determine its age: replicative life span (RLS) and chronological life span (CLS) [45]. The chronological lifespan (CLS) is a measure for the time a non-dividing cell can survive and keep its ability to return into a dividing stage. The RLS reflects the number of "daughter" cells that are budding of one "mother" cell, and thus resembles the aging of mammalian cells that undergo a fixed number of divisions before dying (such as fibroblasts). While there are technical approaches to determine the CLS in high-throughput, the RLS is still mainly analyzed using a manual method that was already introduced in 1959 [46]. The laborious and low-throughput methods of current yeast RLS assays limit their usefulness as a model for research on aging.

To determine the RLS manually (Fig. 1.A), the yeast strain of interest is streaked from a frozen stock onto an agar plate. After colonies have formed, they are used to inoculate a fresh plate containing the same growth medium. This main cultivation plate is incubated until colony formation can be detected. About 40–60 single cells are picked from the

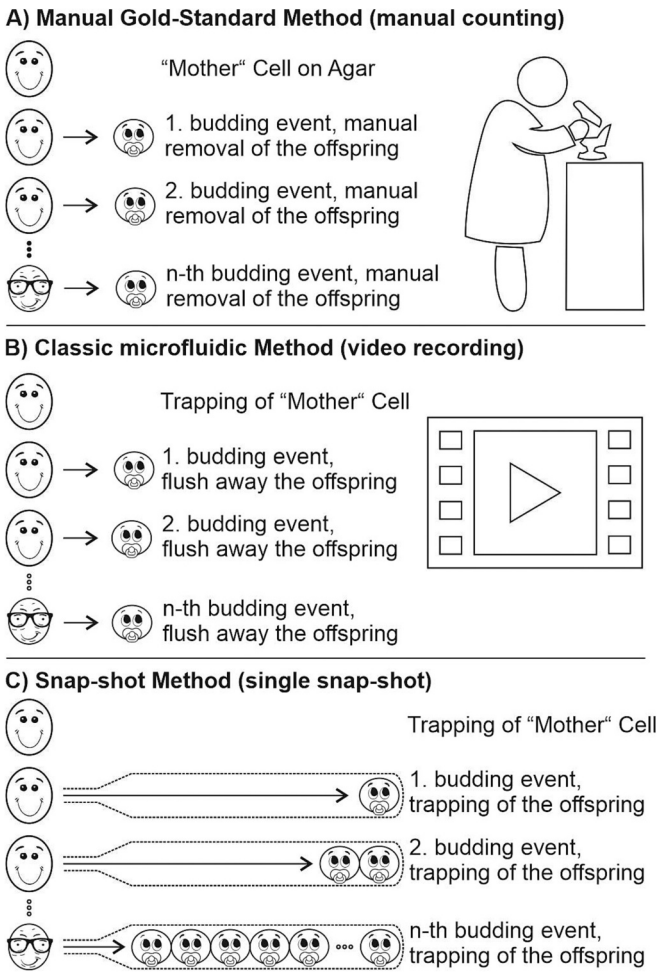

Fig. 1. Comparison of different approaches for RLS determination: A) Manual determination via microdissection, B) Microfluidic approach through trapping a mother cell and removing the offspring while taking a video subsequent counting, C) HAPPY approach employing special defined trapping of mother and daughter cells and single snapshot determination.

patch of cells using a micromanipulation microscope and transferred to defined coordinates on the same plate. The plate is further incubated until the isolated cells divide for the first time after they have been transferred.

"Mother" and "daughter" cells are separated from each other using the micromanipulator again, and while the "daughter" cell remains at the initial coordinates of its "mother", the "mother" cell is being removed and discarded. The number of "daughter" cells deriving from this "virgin" cells is counted by incubating the plates for intervals of 90–120 min, interrupting the incubation, separating the cells from their own "daughter" cell, discarding this new "daughter" cell, and continuing the incubation.

Considering that a typical RLS of a yeast strain could range from 20 to 60 divisions, on average an experiment can run over 15 days, where every 60–90 min a manual intervention is needed for separating the "mother" and "daughter" cells for continuous tracking of "mother" cells (during an eight-hour workday, the described procedure is repeated between four and six times, before the plates are stored at 4 °C to slow down the cell division overnight).

The idea to overcome the limitations of manual lifespan determination employing microfluidics is not innovative as such. Since 2012, a number of research groups have published microfluidic based cultivation devices, which allow the measurement of the RLS with an (compared to the manual method described above) increased throughput.

The devices feature clever geometrical structures to mechanically (or chemically) trap "mother" cells. While the "mother" cell is trapped, the offspring is flushed away and can be quantified based on a time-lapsed microscopic video after the experiment is over. Trapping mechanisms employ a variety of approaches featuring functionalizing the glass surface of a microfluidic device with biotinylated bovine serum albumin followed by neutravidin and thus, trapping biotin labelled ("mother") cells [47,48], vertical trapping by manipulation the floor-to-ceiling distance in the device during the inoculation (temporarily) by increasing the pressure in the device and trapping cells by pressure release beneath the lowering "collapsing" ceiling [49,50], cavity trapping in dead-end tips [51], and most commonly horizontal mechanical trapping [52–54] which is also used in the here described concept.

What all published methods do have in common is the requirement for sophisticated microfluidic equipment, and experienced personnel who are adept at using the microfluidic chips. Especially the need for time-lapse high spatial and temporal resolution microscopy for monitoring single cells is in our opinion the main reason why these devices never achieved to widely replace the manual gold-standard-method for RLS determination.

By designing the device described below, we aim for a microfluidic chip capable of overcoming these challenges by focusing on both "mother" and "daughter" cells, and by relying on snap-shot photography rather than on video imaging. Due to the hierarchic design of the chip, the RLS of a single yeast cell can be deduced by counting of the total number of "daughter" cells trapped after the trapping and cultivation of a "mother" cell. The design of the device necessitated the precise and accurate fabrication of multiple microfluidic features with a high aspect ratio.

Typically, a RLS yeast determination experiment lasts 2–3 weeks resulting in really low throughput [55] whereas a typical microfluidic-based RLS experiment lasts 2–5 days [56]. A recent review by Chen et al., reports that the yeast cell retention within the traps ranged from 15% to 90%, whereas the number of strains tested by device ranged from 1 to 8 [56]. On the other hand, the HYAA chip reported a retention efficiency of up to 96% with the possibility to trap up to 8000 cells, and testing up to 16 samples corresponding to different strains. More recently, Wang et al. reported a trapping efficiency ranging from 70% up to 92% after 4 h of cell loading with the possibility to test up to 5 strains [57]. In 2022 another work from Thayer et al. presented a design featuring 24 independent channels allowing for 24 experiments with 800 traps approximately in each channel but no data on retention efficiency is mentioned [58]. Duran et al. presented a microfluidic device featuring three independent channels with a retention rate ranging from 25% to 55% [59].

Here we demonstrate the feasibility of fabricating such a microfluidic device by means of photolithography comprising a single cell trap, a delay structure and a chamber defined by micropillars. The novelty of the present work lies in the integration of the above-mentioned microfluidic structures into a single device by means of the established method of photolithography, the fine-tuning of essential parameters to achieve the desired high aspect ratio (1:5) and the use of commercially available resins. The fine-tuning of the fabrication parameters in combination with the selection of the appropriate resin allowed for the reproducible patterning of micron-sized features. Instead of using sophisticated time-lapse microscopy, we present a design allowing for determination of the number of "daughter" cells produced by single "mother" cells by taking a single snapshot of specific areas of the microdevice at the end of each experiment. To our knowledge, we are the first to propose this type of configuration for RLS determination.

2. Materials and methods

2.1. Microfluidic device design

The microfluidic device used in the presented work was designed to allow the determination of the RLS of budding yeast cells (number of "daughter" cells coming from one "mother" cell), without requiring sophisticated microfluidic infrastructure or motorized microscopes (or sample platforms). To do so, yeast cells and their offspring are trapped in defined locations on the device, facilitating the counting of said offspring and thus, allowing for the determination of the RLS by taking only one picture at the end of the cultivation. The novel concept and the corresponding innovative combination of microfluidic features of the device are described in detail in the next section. In brief, the microfluidic design comprises two single cell traps, a delay structure, and a collection chamber.

2.2. Device fabrication

The careful fine-tuning of the chip fabrication was necessary to ensure the functionality of the microdevice and the parameters are one of the results of the study presented here. Thus, the production process is described in detail in the Results section. In short, the microdevices are fabricated in silicon wafers by means of photolithography followed by a plasma etching step. The bonding process to form enclosed channels is

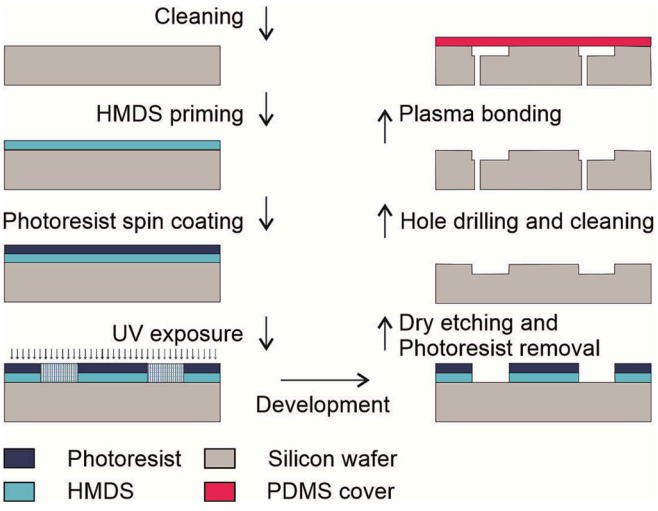

Fig. 2. Fabrication process flow of the microfluidic device.

achieved by PDMS bonding. Fig. 2 shows the fabrication process flow. The workflow of the whole approach from conceptualization to realization to validation is provided in Fig. S1.

2.2.1. Cleaning process

Prior to using the wafers, extensive cleaning was performed to remove any contaminants and/or particles that may have been deposited on the wafer surfaces. Thorough cleaning proved to reduce the probability of defects in the final fabricated product. The cleaning process consisted of 5 steps: 1) 5 min sonication in distilled (DI) water, 2) 5 min sonication in acetone, 3) 5 min sonication in isopropanol (followed by a second wash if needed), 4) drying using only a nitrogen gas air gun, 5) perform oxygen (O_2) plasma etching (Oxygen Plasma cleaner -MARCH O_2 PLASMA system) for 15 min (settings: RF power of 150 W Forward & 1 W reflected, O_2 gas between 450 and 600 mTorr).

2.2.2. Photolithography

Positive photolithography was performed using Shipley 1813 photoresist (Microposit S1800 series, Kayaku advanced materials). The clean wafer was placed on the spin coater (Headway Research Inc.). Using a clean pipette tip, 0.5 ml of hexamethyldisilazane (HMDS) solution were casted and spun at 4000 rpm for 40 s to increase the adhesion of the photoresist on the silicon wafer surface. After ensuring that 80% of the surface was covered with HMDS by visual inspection, another 1 ml of Shipley 1813 photoresist was cast and spun at 4000 rpm for 40 s using a clean pipette tip. The coated wafer was placed on a clean hot plate (Thermo Fischer Scientific Inc.) for a pre-exposure (soft) bake at 100 °C for 60 s.

A Karl Suss MA4Mask aligner was used for the exposure. The quartz-chromium mask was placed on the mask holder and the glass slides were aligned to the mask. Vacuum contact was engaged during exposure to provide good contact. The exposure time was 6 s.

The development step was carried out using a MF-CD-26 Developer, by dipping and softly agitating the wafers in the developer for a minimum of 30 s or until the resist was dissolved off the surface completely. Afterwards, the wafers were immediately transferred to DI water and gently agitated. The wafers were gently rinsed with DI water and then dried under a stream of nitrogen. Subsequently, they were placed on a clean hot plate (Thermo Fischer Scientific Inc.) and hard baked at 120 °C for 10 min prior to DRIE etching.

2.2.3. DRIE process

The Surface Technology Systems (STS) Deep Reactive Ion Etcher (DRIE) was used for the silicon etching procedure. The silicon wafers, processed through photolithography as described above, were loaded into the STS system, and exposed to SF6 etch at 130 sccm, with C4F8 passivation at 85 sccm and an O2 cleaning etch at 13 sccm as a cleaning step. The total exposure time was 3.54 min, corresponding to 14 cycles of exposure, passivation, and cleaning. Post-exposure cleaning involved immersing processed wafers into PG Remover (photoresist remover, Kayaku Advanced Materials) for 5–10 min to dissolve the photoresist. PG remover was rinsed off in isopropanol and the wafer was dried under nitrogen gas. Wafers were cleaned by immersion in Piranha acid solution for 15 min to remove trace amounts of photoresist.

2.2.4. Bonding process

2.2.4.1. Preparation of PDMS solution. The PDMS solution was prepared by mixing the base and curing agent according to the manufacturers (Sylgard 184, Dow Corning) recommended mixing ratio (10:1 ratio of base to curing agent by weight). The solution was mixed well using a clean 20 ml syringe or a clean mixing spoon and finally the PDMS mix was desiccated for at least 30 min to an hour to remove all air bubbles.

2.2.4.2. PDMS casting. While the PDMS was degassing, the casting frame and silicon master wafer were prepared (in our case a silicon wafer with no features on it). The silicon wafer was gently cleaned with an air gun. The silicon wafer was placed in the casting frame and prepared for PDMS injection. A 60 ml syringe was used and the PDMS was very gently injected into the casting frame. The PDMS was baked for 1–2 h at 80 °C (according to manufacturer's instructions, Sylgard 184). Once baked, the PDMS was demolded from the silicon wafer.

2.2.5. Plasma bonding

A PE-50 plasma bonder (Plasma Etch Inc., Nevada, USA) was used at the following settings: RF power adjusted to FWD/REF 15 W/0 W for 30 s, oxygen tank set to 15 psi, vacuum adjusted to 250 mTorr. To ensure smooth operation of the PE-50, the system was left under vacuum for a minimum of 15 min before exposing the device surfaces (Supplementary Table 1). The channel layer (facing up) and membranes were exposed at the intended exposure rates and for the appropriate time. The chips and membrane wafers were removed quickly from the plasma etching system once the cycle was complete and the channel layer was bonded to the channel layers within the first minute. Then the wafer was placed inside the vacuum oven at 60 °C for 10 min.

2.2.6. Laser dicing process

To cut each device according to the preselected dimensions from the wafer, a 355 nm laser dicing system (Potomac Photonics Inc.) was used. Prior to laser dicing, the same cleaning process as 3.2.2 was followed. A protective acrylic coating (acrylic conformal coating 2108-12S) was sprayed on the surface of the wafer prior to the dicing step. The wafer was then diced into individual devices according to the file introduced containing all the dimensions needed for a precise cut. Once the dicing was completed, the individual devices were placed in a Coplin jar in a high frequency (80 Hz) sonicator, first in acetone, then in isopropanol (5 min in each solvent).

2.3. Experimental setup

The experimental set-up consisted of a pumping system (peristaltic pump by Jobst Technologies or syringe pump by *New Era Pump Systems, Inc.*.), a temperature-controlled incubator (Edmund Bühler GmbH), a modular microscope (Resolv4k, Navitar) connected to a light source (coaxial LED illuminator coupled with a desktop controller, Navitar), a high-resolution camera (Pixelink), an xyz stage (Thorlabs) and a personal computer (Fig. 3).

2.4. Yeast culture and inoculation of the chip

The yeast cultures were prepared using Yeast Extract–Peptone–Dextrose (YPD) medium with the pH set at 5.5. In a 1000 ml flask, 100 ml of YPD were inoculated with 100 μl of the BY4741 yeast glycerol stock. The yeast cultures were grown at 30 °C for 17-19 h within a shaking incubator. A Coulter Counter (Beckman Coulter, Inc.) was used to determine the number and the size of the cells within the sample. Culture aliquots were diluted in YPD to a cell concentration of 102–103 cells/ml.

The yeast cultures were prepared using Yeast Extract–Peptone–Dextrose (YPD) medium with the pH set at 5.5. In a 1000 ml flask, 100 ml of YPD were inoculated with 100 μl of the BY4741 yeast glycerol stock. The yeast cultures were grown at 30 °C for 17–19 h within a shaking incubator. A Coulter Counter (Beckman Coulter, Inc.) was used to determine the number and the size of the cells within the sample. Culture aliquots were diluted in YPD to a cell concentration of 102–103 cells/ml before introduction into the chips to perform further experiments.

Before starting each experiment, the chips were primed with 1% polyethylene glycol (PEG) solution to passivate and hydrophilize the interior of the chip and enable a uniform filling of the chip. This step was performed with a flow rate of 1–10 μl/min for 15 min. The diluted yeast

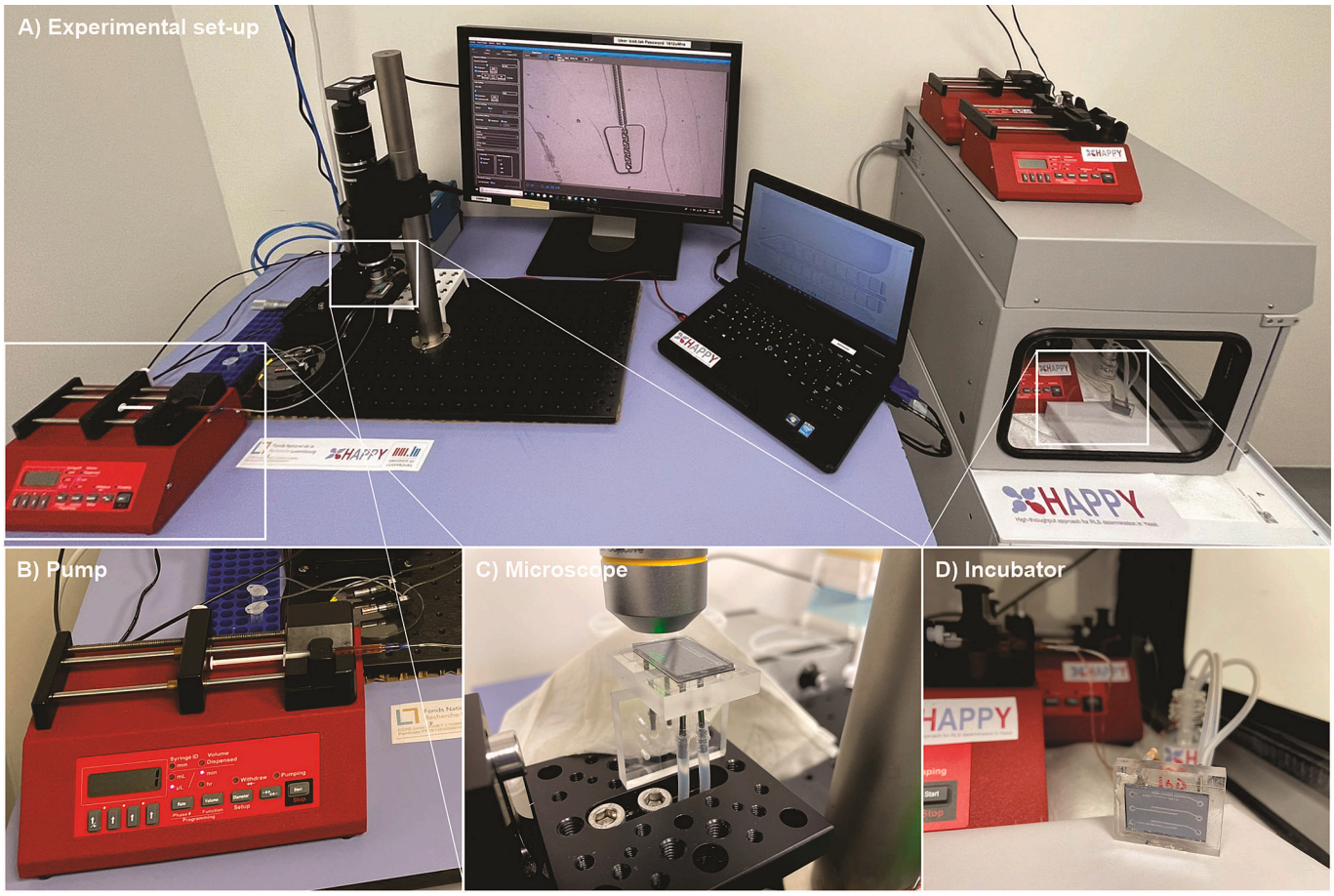

Fig. 3. Experimental Set-up: Yeast cultivation or inoculation medium is pumped into several microfluidic devices at the same time, while the devices are kept at 30 °C using a temperature-controlled incubator. For visual inspection, the devices were taken from the incubator, and placed on the xzy stage. During the whole experimental process, the continuous flow was ensured using a pumping system (syringe or peristaltic).

suspension samples were introduced into the chip at a flow rate of 1–5 μl/min. The step was monitored visually, observing the trapping events using the modular microscope. The inoculation duration varied, according to the time needed to achieve a cell trapping efficiency higher than 50% (minimum eight out of the fifteen single cell traps filled), at least 30 min were needed. Once these cells were captured in the single cell traps, the feeding solution was changed to fresh, cell free YPD medium and the inoculated chip was placed in the incubator. The feeding of cell free YPD medium was continuous for the whole duration of the experiment at a constant rate in the range of 1–3 μl/min.

2.5. Profilometry

Profilometry is a technique used to extract topographical data from a surface such as surface roughness and texture. A scanning probe scans through contact or non-contact methods the surface and collects topographical information through high-precision data acquisition components. It is a powerful tool for characterizing microfluidic devices, as the profile generated can reveal fine details not visible with traditional optical microscopy. In our case, we used the profilometer (Dektak®) to measure step heights across sections of the device during the fabrication process as well as the final height of the microfluidic features.

2.6. Scanning Electron microscopy (SEM)

Scanning electron microscopy (SEM) is a powerful analytical tool that can be used to characterize microfluidic devices. SEM enables a high-resolution three-dimensional analysis of the physical characteristics of microfluidic devices, including the dimensions, surface features, and internal structures. In this study SEM (Hitachi S-3400 variable pressure SEM) was employed to measure the dimensions of microfluidic features with high precision.

2.7. Pressure drop measurements

The pressure drop across a microfluidic device is a key measure of the performance of these systems. The pressure drop of a microfluidic device can be determined by measuring the pressure at different points in the device as a function of the flow rate. To do this, a pressure driven pump was used to create a constant flow rate through the device. At each flow rate, the pressure was measured at both inlet and outlet ports, and the difference in pressure is used to calculate the pressure drop. This method can be used to accurately determine the pressure drop across a microfluidic device for various flow rates. The tests were conducted at different flow rates ranging between 1 μl/min and gradually increased to 25 μl/min. The pump's (Fluigent, Flow EZ) maximum pressure range is 2000 mbar. Therefore, the pump was run at a maximum of 1800 mbar for 2.5 min until we began gradually reducing the air pressure.

3. Results

3.1. Concept

As described above, all published microfluidic devices for RLS determination require the use of sophisticated microfluidic infrastructure, motorized microscopes (or platforms), and software solutions for

the interpretation of large video data sets (Fig. 1). Within this study, we were aiming for a microfluidic concept that could be realized without requiring this infrastructure and thus, could be established in a yeast lab without microfluidic expertise.

Towards this aim we envisioned a design allowing for the determination of the RLS based on solely one microscopic picture. Hence, our design needed to ensure the trapping and localization of both the "mother" and the "daughter" cells, as well as a technical solution for removing the offspring of the "daughter" cells.

To achieve the desired trapping and localization of cells in specific positions within the chip, we had to combine three different microfluidic structures in one chip, namely single cell traps, delay structures, and collection chambers made of pillars.

According to the concept depicted in Fig. 1C), single cells of unknown age ("grandmother cells") are supposed to be randomly trapped in the first single cell trap during the inoculation phase. After switching the cell containing inoculation medium to cell free cultivation medium, the trapped "grandmother" cells start dividing and the first offspring of each "grandmother" cell is supposed to be trapped in the second single cell trap ("mother" cell). The size and depth of the single cell traps have been optimized according to the mature size of the used yeast strains (BY4741), to ensure that only one cell fits in each single cell trap.

After a successful trapping event of a ("virgin") "mother" cell, the entire offspring of this cell is trapped in a linear way in the pillar structure adjacent to each "mother" cell. To allow for the offspring of each "mother" cell to grow in size before being trapped, the "mother" and "daughter" cell traps are interspaced by a herringbone-like delay structure.

The pillar structure is designed in a way that allows the offspring of trapped "daughter" cells to escape the trap. Thus, preventing false positive counting events.

3.2. Microfluidic design

Before reaching the current design, our group experimented with several designs. During the first generation of chips (Supplementary Fig. S3) which consisted of two single cell traps, two delay structures (one wide chamber and a meandering channel respectively) and a pillar structure de-fining the collection chamber, we did not manage to run experiments due to the poor robustness and the insufficient reproducibility of the chips. These chips were fabricated in PDMS. For the second generation of chips (Supplementary Fig. S4), we tried to simplify the design to achieve better reproducibility and study parameters such as the size of the traps and the shape of the de-lay structure. The second generation comprised a single cell trap, a delay structure and a chamber defined by pillars. In the second generation three different shapes for the delay structure where investigated: meander shaped, herringbone shaped and kidney shaped (Supplementary Fig. S5). This chip was fabricated in silicon. Both generations had 3 channels each featuring 15 unit cells arranged orthogonally to the direction of the flow.

The current version of the device features structures for the trapping of single cells (single cell traps), and their offspring (pillar structure). In addition, it requires structures that allow slowing down the movement of newly generated (small) cells through the device, so that these cells can be trapped after reaching a mature size (delay structures). The dimension of the device is 2.6 cm by 1.7 cm. Each device consists of three identical, independent channels allowing to perform three experiments simultaneously, employing either different conditions or different strains. Each channel is rhombus shaped with a total length of 2.2 cm and contains a single inlet and outlet (5 mm apart). Each channel accommodates fifteen unit-cells with a total length of 740 μm. Each unit cell comprises two single cell traps and a collection chamber defined by pillars where the offspring of one "mother" cell is collected. Between the second single cell trap ("mother" cell trap) and the collection chamber ("daughter" cell trap), a delay structure is included.

The pillar structures defining the collection chamber have a width of 3 μm, a length of 5 μm and a pitch of 6 μm, respectively. The spacing (3 μm) between the pillars allows the offspring of the "daughter" cells to be flushed away towards the outlet in order not to interfere with the total cell counting stemming from the trapped "mother" cell. The width of the collection chamber is 8 μm with a total length of 600 μm. A schematic representation of the device with a zoom-ups of the unit cell with annotated dimensions is illustrated in Fig. 4 (see also Supplementary Fig. S2).

Computer-aided design software (AutoCAD) was used to create precise 2D drawings for the photolithography mask design which were subsequentlyused for the fabrication of the photolithographic quartz-chromium masks (Fig. S2). The fabrication of the photolithographic mask was outsourced to Photomask Portal (https://www.photomaskportal.com/).

In comparison to the final design, the first delay structure of the first generation was found redundant leading to its elimination. As for the second generation in comparison to the first one, the shape, size and orientation of the pillar structures were optimized. The optimized pillar structures (bigger in size by 1 μm and tilted with regards to the direction of the flow) were incorporated in the final design. In comparison to the final design, the second design did not feature a "grand mother cell" trap in order to simplify the design and its fabrication complexity. In the final design the unit cells were placed in an open diamond shape chamber instead of having them arranged orthogonal to the direction of flow and connected to the common inlet and outlet channels. The second design created unpredicted flow directionalities and caused a high backpressure in the chips. By placing the unit cells in a diamond shaped chamber, the flow was smoother, and the backpressure was reduced.

3.3. Technical validation

Prior initiating the biological validation experiments, an extensive characterization of the fabricated microdevices was performed in terms of fabrication accuracy, flow, and pressure.

3.3.1. Fabrication accuracy

Scanning electron microscopy (SEM) was employed to characterize the interior of the fabricated microdevices as shown in Fig. 5 (see also Supplementary Fig. S6). The microfluidic features were patterned sharply, providing clear feature edges despite the high aspect ratio. The fabrication accuracy was higher than 85% and 93% for features smaller than 3 μm and 5 μm, respectively (Supplementary Table 2).

A profilometer was used to measure the height of the features, the thickness of the photoresist prior to DRIE etching as well as the depth of the fabricated channels. A typical thickness of the spin coated resin was approximately 1.6 μm. Depending on the number of DRIE cycles applied, different channel depths were achieved ranging from 10.8 to 16.5 μm corresponding to 14 and 23 DRIE cycles, respectively. As the desired channel depth was 10 μm, we decided to apply 14 cycles, which were completed within 3.54 min (Supplementary Table 3).

3.3.2. Flow and pressure

Backpressure measurements were performed at different flowrates to determine the leak-tightness of the fabricated chips. Flow rates ranging from 1 to 25 μl/min were applied through a pressure driven pump (Fluigent, Flow EZ) and the pressure generated within the device was measured. The range of flow rates for this test was selected according to the needs of the planned biological assays based on the existing literature [60]. The relation between the volumetric flow rate applied and the measured pressure is depicted in Fig. 6. According to these measurements, the microdevices proved to be robust and demonstrated stable performance when operated with flow rates of 25 μl/min, which is also translated in pressure drops higher than 1750 mbar. During these tests, no leakages were observed, indicating a good robustness of our fabricated microdevices.

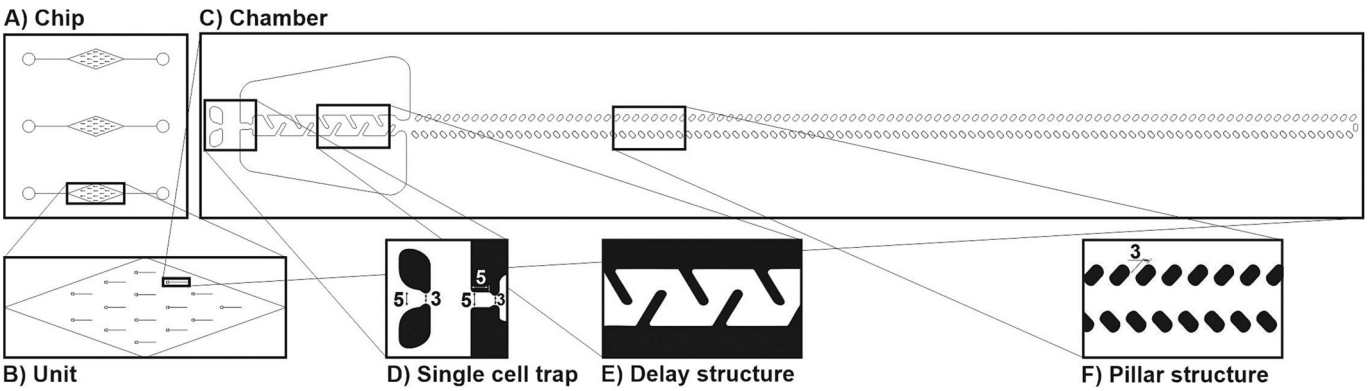

Fig. 4. Schematic overview of the microfluidic design: A) Device, featuring three individual channels with one inlet and outlet per channel, which allows to perform three independent experiments in parallel (e.g., different media or yeast strains. B) Enlarged channel, showing the rhombus/diamond shape design with 15-unit cells (pes channel) arranged parallel to the direction of the flow. C) Enlarged unit cell, comprised of two single cell traps ("grandmother" and "mother" cell trap), a (herringbone-shaped) delay structure designed to decrease the progress of newly created cells through the device to allow for the cells to grow in size, and a collection chamber defined by a pillar structure designed to trap all offspring of the cell trapped in the second single cell trap ("daughter" cell trap). D) Enlarged single cell traps. E) Enlarged delay structure. F) Enlarged pillar structure.

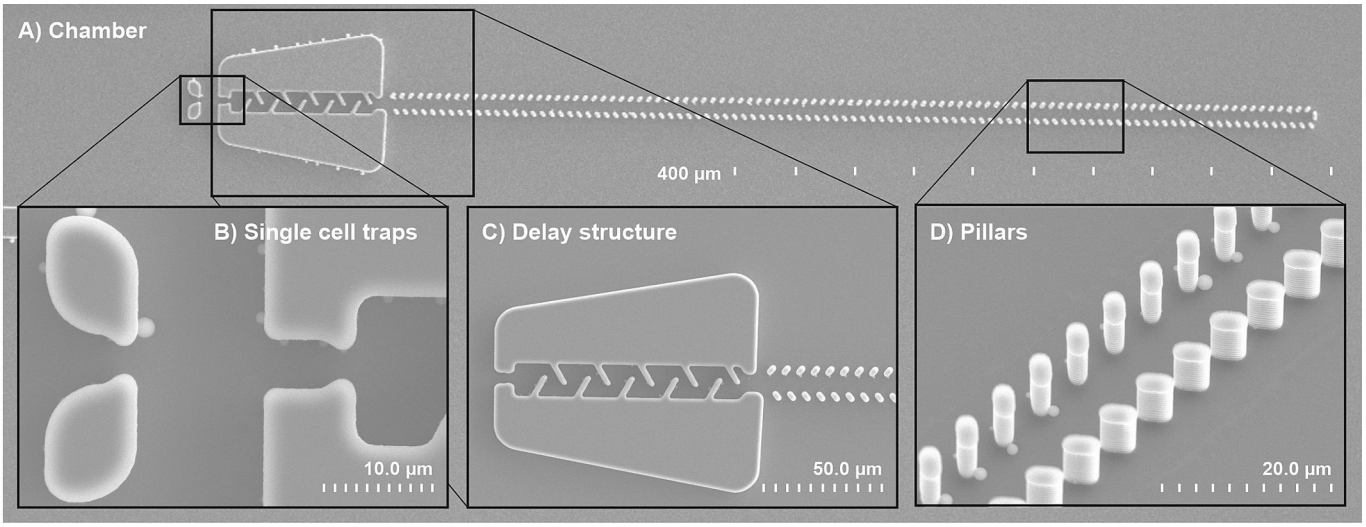

Fig. 5. Scanning electron microscopy (SEM) pictures taken from the fabricated devices. A) Chamber (by FABLAB 15.0 kV 10.0 × 130 SE). B) Single cell traps (by FABLAB 15.0 kV 10.0 × 3.2 SE). C) Delay structure (by FABLAB 15.0 kV 10.0 × 7000 SE). D) Pillars (by FABLAB 15.0 kV 9.8 × 2.5 SE).

3.4. Experimental validation

3.4.1. Yeast culture size validation

As the separation of different cell types is achieved solely based on their diameter, the choice of the trap dimensions as well as the control of the single cell sizes were of high importance. Thus, the preparation of the yeast inoculum was standardized, and followed a protocol that was also used to determine the average size of the used yeast strain, BY4741. The single cell size of 4.7 ± 0.05 µm (Fig. S7) in the mid-exponential growth phase was determined as an average value in five independent cultivations carried out at glucose concentrations between 1 and 10% (representing the most commonly used concentrations in literature).

Based on this value, we designed the single cell traps to the dimensions of five-by-five µm with a narrowing of 3 µm. The selected dimensions would allow only one cell to be trapped but would still be big enough to allow for the cell to role, to turn a new bud into the direction of the flow without being washed out of the trap.

3.4.2. Device validation

To validate the technical functionality of the chip, we performed yeast trapping experiments according to the protocol described above (section 2.4). The continuous flow was ensured for the whole duration of the experiment through a peristaltic or a syringe pump (per channel). Specifically, we were assessing the following functionalities: trapping of single cells in the single cell traps; effect of the delay structure on the movement speed of single cells; trapping of "daughter" cells by the pillar structures; escaping of the offspring of "daughter" cells through the gaps between the pillar structures. As we did not monitor the chips in a continuous fashion, our observations are limited to the pictures taken at the beginning and end of each cultivation. Still, we were able to capture trapping events in the first and second single cell traps, linear trapping events of multiple cells, and budding events from both single and multiple cell traps. Fig. 7 depicts selected pictures of the said events. As for the retention performance of our device, it is capable of reaching 50% within 30 min of feeding. Concerning the throughput, three strains can be simultaneously tested per device.

4. Discussion

In this study, we present a novel design for a microfluidic system which could form the basis for developing a more rapid and facile analysis of the yeast RLS. Unlike the previously described microfluidic

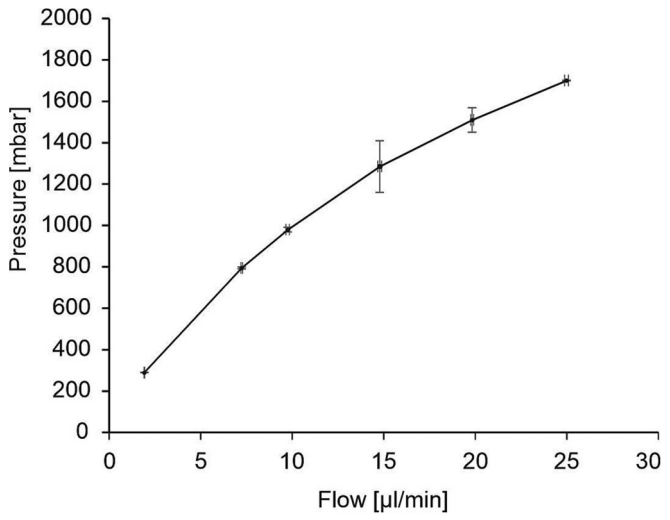

Fig. 6. Pressure in mbar against flow rate in µl/min: Each flow rate has been applied for a minimum of 20 s. During the test, the device showed no leakages.

systems used for yeast RLS assays, relying on time-lapse microscopy, we envisage a microfluidic approach allowing for RLS determination through a single snapshot at the end of the experiment for counting all the "daughter" cells, produced from a single "mother" cell, aligned in the collection chamber.

Here, we present the feasibility of producing the desired microfluidic devices by means of photolithography and plasma etching, employing commercially available resin, and by fine-tuning the parameters of the fabrication process to achieve the demanding features of our microfluidic design. Using the fabricated devices, we demonstrated the functionality of the features of our design including the single cell trapping of yeast cells, the capturing of the "daughter" cells in the collection chamber as well as the flushing away of their offspring towards the outlet.

Currently, we are optimizing the described device to eventually implement the simplified yeast RLS assay via single snapshot, as described above.

Despite the successful fine-tuning of the chip fabrication process, we encountered challenges during the biological validation of the chip (low reproducibility of trapping efficiency, multiple trapping events in "mother" cell traps, "mother" cells being flushed away during cultivation, clump formation of "daughter" cells in the pillar structure). Thus, we expect the necessity of optimization steps before being able to provide a sufficient reproducibility to fully replace the manual gold standard method using our device.

Already during the technical test phase, which resulted in the design presented here, we encountered problems related to the backpressure, the directionality and the regularity/smoothness of the flow while realizing our conceptual design. Regarding the backpressure, minimal changes to the design (positioning of structures towards the directionality of the flow) were implemented aiming at decreasing the pressure drop. In addition, eliminating structures that proofed to be not essential (flow guidance barriers) were removed. In a previous design, the device described here (while following the same concept) was comprised of several parallel chambers connected to central in- and outlet cannels. Arranging the single chambers within a rhombus shaped chamber alleviated the pressure drop. In order to tackle the directionality and smoothness of the flow, we are exploring the use of different pumping systems. Both displacement (i.e., syringe/peristaltic) and pressure driven pumps will be evaluated so as to achieve the ultimate goal which is a smooth and well controlled flow allowing for a uniform filling of the microdevice, which in turn will potentially lead to increased single cell capturing efficiency.

A promising new methodology of a fabrication of reproducible and

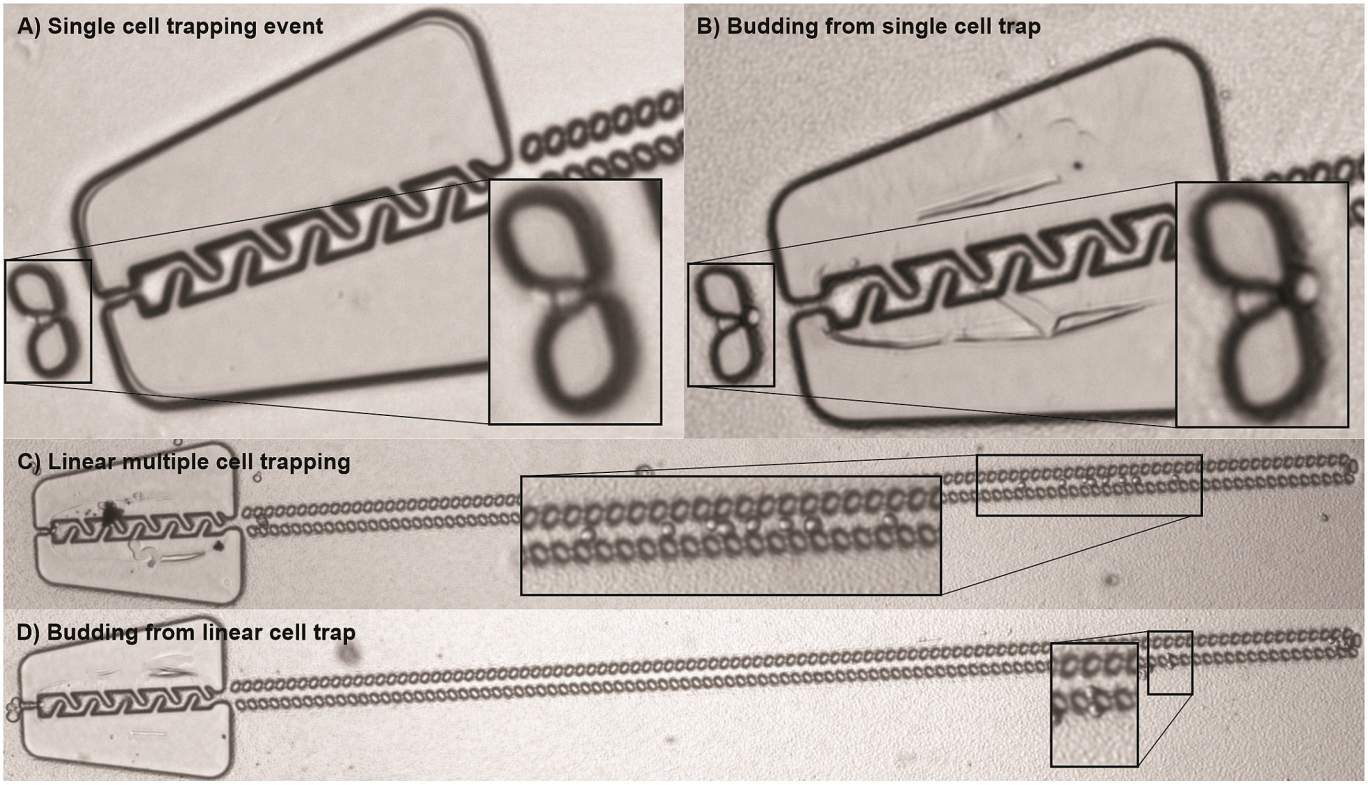

Fig. 7. Cell trapping and budding events: A) Single cell trapped in the first single cell trap (45× magnification, Navitar), B) Budding event from a single cell trap (45× magnification, Navitar), C) Multiple "daughter" cells trapped in the pillar structure and arranged in a linear fashion (25× magnification, Navitar), D) Budding event from trapped "daughter" cells with offspring escaping through the pillar structure (25× magnification, Navitar).

reliable high aspect ratio features in a microfluidic system for trapping, cultivating, and counting cellular material has been demonstrated. This fabrication protocol can be widely utilized for other microfluidic applications where high aspect ratio features are routinely employed such as pillar arrays, droplet generators, mixers, etc. In this study, we applied the protocol to produce microfluidic chips for fast and simple determination of yeast replicative lifespan. After further optimization towards the RLS assay, this device could greatly accelerate research on aging mechanisms in eukaryotic cells and make yeast replicative lifespan determination amenable to many more laboratories, both in academia and industry.

5. Patents

MICROFLUIDIC SYSTEMS FOR YEAST AGING ANALYSIS, Inventors: PACZIA NICOLE [DE]; JUNG PAUL [FR]; SHAH PRANJUL [IN]; DIMAKI MARIA [DK]; SVENDSEN WINNIE EDITH [DK]; LINSTER CAROLE [LU] Publication: US2021198608A1·2021-07-01 [61].

Funding

This research was supported by the Luxembourg National Research Fund (FNR) through a Proof-of-Concept grant (PoC19/13593527 - HAPPY) to CLL.

Supplementary data to this article can be found online at https://doi.org/10.1016/j.mne.2023.100199.

Declaration of Competing Interest

The microfluidic replicative lifespan detection chip described in the paper is part of the intellectual property covered by the patent [US2021198608A1].

The authors declare that they have no known competing financial interests or personal relationships that could have appeared to influence the work reported in this paper.

The authors declare that they have no competing/conflicting interests.

Data availability

Data will be made available on request.

Acknowledgments

We would like to give special thanks to John Abrahams, Jonathan Hummel, Thomas Loughran, and Mark Lecates at the University of Maryland Nanocenter for their guidance and advice through the course of this effort. We would also like to acknowledge Michael Davis, Petra Walker, Angela Walker and Michael Tolosa at Potomac Laser for their assistance during device development. We would like to thank the Fablab of the University of Luxembourg Incubator for access to Form2 3d printer. Finally, we would like to thank Dean Cheung for technical help with yeast cultivations.

References

[1] P. Gravesen, J. Branebjerg, O.S. Jensen, Microfluidics-a review, J. Micromech. Microeng. 3 (4) (1993) 168–182.
[2] S.F. Berlanda, et al., Recent advances in microfluidic Technology for Bioanalysis and Diagnostics, Anal. Chem. 93 (1) (2021) 311–331.
[3] K.W. Oh, Multidisciplinary role of microfluidics for biomedical and diagnostic applications: biomedical microfluidic devices, Micromachines 8 (12) (2017) 343.
[4] K.W. Oh, Microfluidic devices for biomedical applications: biomedical microfluidic devices 2019, Micromachines 11 (4) (2020) 370.
[5] L.Y. Yeo, et al., Microfluidic devices for bioapplications, Small 7 (1) (2011) 12–48.
[6] M. Monjezi, et al., Anti-Cancer drug screening with microfluidic technology, Appl. Sci. 11 (20) (2021) 9418.
[7] S. Damiati, et al., Microfluidic devices for drug delivery systems and drug screening, Genes 9 (2) (2018) 103.
[8] C.-M. Chang, et al., Nucleic acid amplification using microfluidic systems, Lab Chip 13 (7) (2013) 1225–1242.
[9] L. Gorgannezhad, H. Stratton, N.-T. Nguyen, Microfluidic-based nucleic acid amplification Systems in Microbiology, Micromachines 10 (6) (2019).
[10] Y. Shen, Y. Yalikun, Y. Tanaka, Recent advances in microfluidic cell sorting systems, Sensors Actuators B Chem. 282 (2019) 268–281.
[11] T. Luo, et al., Microfluidic single-cell manipulation and analysis: methods and applications, Micromachines 10 (2) (2019) 104.
[12] B. Hwang, J.H. Lee, D. Bang, Single-cell RNA sequencing technologies and bioinformaticspipelines, Exp. Mol. Med. 50 (8) (2018) 1–14.
[13] J.F. Hess, et al., Library preparation for next generation sequencing: a review of automation strategies, Biotechnol. Adv. 41 (2020), 107537.
[14] G.-P. Nikoleli, et al., Chapter 13 - biosensors based on microfluidic devices lab-on-a-chip and microfluidic technology, in: D.P. Nikolelis, G.-P. Nikoleli (Eds.), Nanotechnology and Biosensors, Elsevier, 2018, pp. 375–394.
[15] C. Rivet, et al., Microfluidics for medical diagnostics and biosensors, Chem. Eng. Sci. 66 (7) (2011) 1490–1507.
[16] K.F. Lei, Microfluidic Systems for Diagnostic Applications: a review, J. Lab. Automat. 17 (5) (2012) 330–347.
[17] A.-G. Niculescu, et al., Fabrication and applications of microfluidic devices: a review, Int. J. Mol. Sci. 22 (4) (2021).
[18] J. Feng, et al., Microfluidic device based on deep reactive ion etching process and its lag effect for single cell capture and extraction, Sensors Actuators B Chem. 269 (2018) 288–292.
[19] M.-E. Vlachopoulou, et al., Plasma etching of poly(dimethylsiloxane): roughness formation, mechanism, control, and application in the fabrication of microfluidic structures, Plasma Process. Polym. 10 (1) (2013) 29–40.
[20] M. Bu, et al., A new masking technology for deep glass etching and its microfluidic application, Sensors Actuators A Phys. 115 (2) (2004) 476–482.
[21] D.C. Duffy, et al., Microfabricated centrifugal microfluidic systems: characterization and multiple enzymatic assays, Anal. Chem. 71 (20) (1999) 4669–4678.
[22] C. Chen, D. Hirdes, A. Folch, Gray-scale photolithography using microfluidic photomasks, Proc. Natl. Acad. Sci. 100 (4) (2003) 1499.
[23] G.M. Whitesides, et al., Soft lithography in biology and biochemistry, Annu. Rev. Biomed. Eng. 3 (1) (2001) 335–373.
[24] D.A. Mair, et al., Injection molded microfluidic chips featuring integrated interconnects, Lab Chip 6 (10) (2006) 1346–1354.
[25] H. Becker, U. Heim, Hot embossing as a method for the fabrication of polymer high aspect ratio structures, Sensors Actuators A Phys. 83 (1) (2000) 130–135.
[26] R. Suriano, et al., Femtosecond laser ablation of polymeric substrates for the fabrication of microfluidic channels, Appl. Surf. Sci. 257 (14) (2011) 6243–6250.
[27] A.K. Au, et al., 3D-printed microfluidics, Angew. Chem. Int. Ed. 55 (12) (2016) 3862–3881.
[28] C.M. Sotomayor Torres, et al., Nanoimprint lithography: an alternative nanofabrication approach, Mater. Sci. Eng. C 23 (1) (2003) 23–31.
[29] P. Mali, A. Sarkar, R. Lal, Facile fabrication of microfluidic systems using electron beam lithography, Lab Chip 6 (2) (2006) 310–315.
[30] R.H. Stulen, D.W. Sweeney, Extreme ultraviolet lithography, IEEE J. Quantum Electron. 35 (5) (1999) 694–699.
[31] K.J. Lawrie, et al., Chain scission resists for extreme ultraviolet lithography based on high performance polysulfone-containing polymers, J. Mater. Chem. 21 (15) (2011) 5629–5637.
[32] G.S. Fiorini, D.T. Chiu, Disposable microfluidic devices: fabrication, function, and application, BioTechniques 38 (3) (2005) 429–446.
[33] J.B. Nielsen, et al., Microfluidics: innovations in materials and their fabrication and functionalization, Anal. Chem. 92 (1) (2020) 150–168.
[34] K.F. Jensen, Silicon-based microchemical systems: characteristics and applications, MRS Bull. 31 (2) (2006) 101–107.
[35] K. Ren, J. Zhou, H. Wu, Materials for microfluidic Chip fabrication, Acc. Chem. Res. 46 (11) (2013) 2396–2406.
[36] A. Manz, N. Graber, H.M. Widmer, Miniaturized total chemical analysis systems: a novel concept for chemical sensing, Sensors Actuators B Chem. 1 (1) (1990) 244–248.
[37] H. Becker, L.E. Locascio, Polymer microfluidic devices, Talanta 56 (2) (2002) 267–287.
[38] M. Rahman, et al., NemaLife chip: a micropillar-based microfluidic culture device optimized for aging studies in crawling C. elegans, Sci. Rep. 10 (1) (2020) 16190.
[39] L.H. Hartwell, Nobel lecture: yeast and cancer, Biosci. Rep. 22 (3) (2002) 373–394.
[40] C.M. Coughlan, J.L. Brodsky, Use of yeast as a model system to investigate protein conformational diseases, Mol. Biotechnol. 30 (2005) 171–180.
[41] A. Nakano, Yeast Golgi apparatus–dynamics and sorting, Cell. Mol. Life Sci. CMLS 61 (2004) 186–191.
[42] K. Bowers, T.H. Stevens, Protein transport from the late Golgi to the vacuole in the yeast *Saccharomyces cerevisiae*, Biochimica et Biophysica Acta (BBA)-Mol. Cell Res. 1744 (3) (2005) 438–454.
[43] S.L. Lindquist, Prion proteins: one surprise after another, Harvey Lect. 98 (2002) 173–205.
[44] H. Karathia, et al., Saccharomyces cerevisiae as a model organism: a comparative study, PLoS One 6 (2) (2011), e16015.
[45] V.D. Longo, et al., Replicative and chronological aging in Saccharomyces cerevisiae, Cell Metab. 16 (1) (2012) 18–31.
[46] R.K. Mortimer, J.R. Johnston, Life span of individual yeast cells, Nature 183 (4677) (1959) 1751–1752.
[47] Z. Xie, et al., Molecular phenotyping of aging in single yeast cells using a novel microfluidic device, Aging Cell 11 (4) (2012) 599–606.

[48] S.M. Rafelski, et al., Mitochondrial network size scaling in budding yeast, Science 338 (6108) (2012) 822–824.
[49] Y. Zhang, et al., Single cell analysis of yeast replicative aging using a new generation of microfluidic device, PLoS One 7 (11) (2012), e48275.
[50] S.S. Lee, et al., Whole lifespan microscopic observation of budding yeast aging through a microfluidic dissection platform, Proc. Natl. Acad. Sci. 109 (13) (2012) 4916–4920.
[51] S. Fehrmann, et al., Aging yeast cells undergo a sharp entry into senescence unrelated to the loss of mitochondrial membrane potential, Cell Rep. 5 (6) (2013) 1589–1599.
[52] C. Jo Myeong, et al., High-throughput analysis of yeast replicative aging using a microfluidic system, Proc. Natl. Acad. Sci. 112 (30) (2015) 9364–9369.
[53] M.M. Crane, et al., A microfluidic system for studying ageing and dynamic single-cell responses in budding yeast, PLoS One 9 (6) (2014), e100042.
[54] P. Liu, T.Z. Young, M. Acar, Yeast replicator: a high-throughput multiplexed microfluidics platform for automated measurements of single-cell aging, Cell Rep. 13 (3) (2015) 634–644.
[55] Au - Steffen, B.K. Au-Kennedy, M. Au-Kaeberlein, Measuring replicative life span in the budding yeast, JoVE 28 (2009), e1209.
[56] K.L. Chen, M.M. Crane, M. Kaeberlein, Microfluidic technologies for yeast replicative lifespan studies, Mech. Ageing Dev. 161 (2017) 262–269.
[57] Y. Wang, et al., A high-throughput microfluidic diploid yeast long-term culturing (DYLC) chip capable of bud reorientation and concerted daughter dissection for replicative lifespan determination, J. Nanobiotechnol. 20 (1) (2022) 171.
[58] H.T. Nathaniel, et al., The Yeast Lifespan Machine: a microfluidic platform for automated replicative lifespan measurements, bioRxiv (2022), https://doi.org/10.1101/2022.02.14.480146, 2022.02.14.480146.
[59] D.C. Durán, et al., Slipstreaming mother machine: a microfluidic device for single-cell dynamic imaging of yeast, Micromachines 12 (2021), https://doi.org/10.3390/mi12010004.
[60] M.C. Jo, L. Qin, Microfluidic platforms for yeast-based aging studies, Small 12 (42) (2016) 5787–5801.
[61] Paczia, N., et al., *Microfluidic systems for yeast aging analysis*. 2021, Google Patents.